

Optical Analysis in $\text{CH}_3\text{NH}_3\text{PbI}_3$ and $\text{CH}_3\text{NH}_3\text{PbI}_2\text{Cl}$ Based Thin-Film Perovskite Solar Cell

Wayesh Qarony*, Yesmin Ara Jui, Gloria Mithi Das, Tashfiq Mohsin, Mohammad Ismail Hossain, Syed Nurul Islam

Electrical and Electronic Engineering, American International University-Bangladesh, Dhaka
*Corresponding author: wayesh@aiub.edu

Received August 18, 2015; Revised August 31, 2015; Accepted September 11, 2015

Abstract The optics of organic-inorganic halide perovskites materials in thin-film smooth surface p-i-n solar cell has been studied. The study was conducted for $\text{CH}_3\text{NH}_3\text{PbI}_3$ perovskite material, used as a photoactive layer and sandwiched between ultrathin electron transport layer of TiO_2 and hole transport layer of P3HT. The investigation was carried out based on the optical wave propagation simulation results of quantum efficiency and short circuit current. A reference model of solar cell exhibits a maximum of 21.79 mA/cm² short circuit current as well as 76% of external quantum efficiency (EQE) for 620 nm to 700 nm of spectral range of wavelengths. Analyzing the influence of thickness for each layer on the short circuit current and the quantum efficiency the cell was optimized. Finally, a comparative analysis has also been done between $\text{CH}_3\text{NH}_3\text{PbI}_3$ and $\text{CH}_3\text{NH}_3\text{PbI}_2\text{Cl}$ perovskite thin-film solar cell, where $\text{CH}_3\text{NH}_3\text{PbI}_2\text{Cl}$ based solar cell gives 2.7% higher short circuit current and around 7.5% higher photon absorption, particularly in the near infrared red regions of spectrum (700 nm- 800 nm) and for the 360 nm of absorbing layer. Throughout the research, a Finite Difference Time Domain (FDTD) based Maxwell's curl equations solver was used.

Keywords: perovskite solar cell, $\text{CH}_3\text{NH}_3\text{PbI}_{3-x}\text{Cl}_x$, quantum efficiency, short circuit current, FDTD

Cite This Article: Wayesh Qarony, Yesmin Ara Jui, Gloria Mithi Das, Tashfiq Mohsin, Mohammad Ismail Hossain, and Syed Nurul Islam, "Optical Analysis in $\text{CH}_3\text{NH}_3\text{PbI}_3$ and $\text{CH}_3\text{NH}_3\text{PbI}_2\text{Cl}$ Based Thin-Film Perovskite Solar Cell." *American Journal of Energy Research*, vol. 3, no. 2 (2015): 19-24. doi: 10.12691/ajer-3-2-1.

1. Introduction

Photovoltaic effect is one of the most effective methods of converting solar energy into electrical energy using solar cells. Although the conventional crystalline silicon or GaAs based single junction solar cells have already been reached to 27.6% of conversion efficiency and multi-junction crystalline solar cell is even more [1], a comparatively very high synthesis and manufacturing costs of photovoltaic cells is limiting the large scale use in real. The necessity of finding high efficiency alternating and cheap sources of energy has made the organometallic halide perovskites (e.g., $\text{CH}_3\text{NH}_3\text{PbI}_3$ and $\text{CH}_3\text{NH}_3\text{PbI}_{3-x}\text{Cl}_x$) based thin-film solar cell as one of the most promising candidate. A very high band-gap, large range of absorption coefficient, light harvesting capability and power conversion efficiency of this new type of solar cells has already surpassed organic and dye-sensitized solar cells. The theoretical efficiency has just incredibly increased from 3.8% to more than 17% in only last couple of 2 years in single and double junction perovskite solar cells [2,3,4,5]. Unlike the organic and dye-sensitized solar cell the perovskite solar cell is non-excitonic due to the lower exciton-binding energy (<50 meV), having ultrafast interfacial charge-transfer speed and electron- and hole-diffusion lengths between 100 nm and a micron [6,7,8].

So, better electrical and optical performances can be achieved for a few more hundreds of nanometers of perovskite geometry.

In this manuscript, the optics in thin-film $\text{CH}_3\text{NH}_3\text{PbI}_3$ perovskite solar cell has been investigated and optimized for the best possible output by analyzing the influence of thickness on upper limit external quantum efficiency and short circuit current. Then a comparative analysis on losses in every layer has also been carried out between $\text{CH}_3\text{NH}_3\text{PbI}_3$ and $\text{CH}_3\text{NH}_3\text{PbI}_2\text{Cl}$ absorbing layer of perovskite thin-film solar cells.

2. Optical Structure Modeling

The optical wave propagation simulations have been performed for thin-film perovskite solar cells on smooth substrate. A schematic cross section of perovskite solar cell on smooth substrate is depicted in Figure 1(a). The perovskite photovoltaic cell structure, investigated in this study, consists of a 130 nm indium tin oxide (ITO) front contact, followed by a 50 nm electron transport layer, TiO_2 , a 360 nm photoactive perovskite material of $\text{CH}_3\text{NH}_3\text{PbI}_3$, a 50 nm hole transport layer of P₃HT (poly (3-n-hexylthiophene)), and a 100 nm Au metal back contact. Simulations were carried out for two dimensional (2D) case, where the simulation environment was created based on finite difference time domain (FDTD) method.

The Maxwell's equations were rigorously solved for the electric field calculation. Since a two dimensional FDTD algorithm was utilized, it splits the Maxwell's equations into two independent sets of equations for transverse electric (TE) and transverse magnetic (TM) polarized waves. The polarization of the input wave was assumed to be TE, thus only one component of the electric field, E_z had to be solved. In order to achieve better absorption,

perfect matched layer (PML) boundary was assumed in z -direction during simulation time. The simulation environment calculates the electrical field inside the proposed structures. In order to obtain the characteristic efficiency parameters in which we were interested, some further processing of this raw data must be performed. In this section, results are shown depending on device structure.

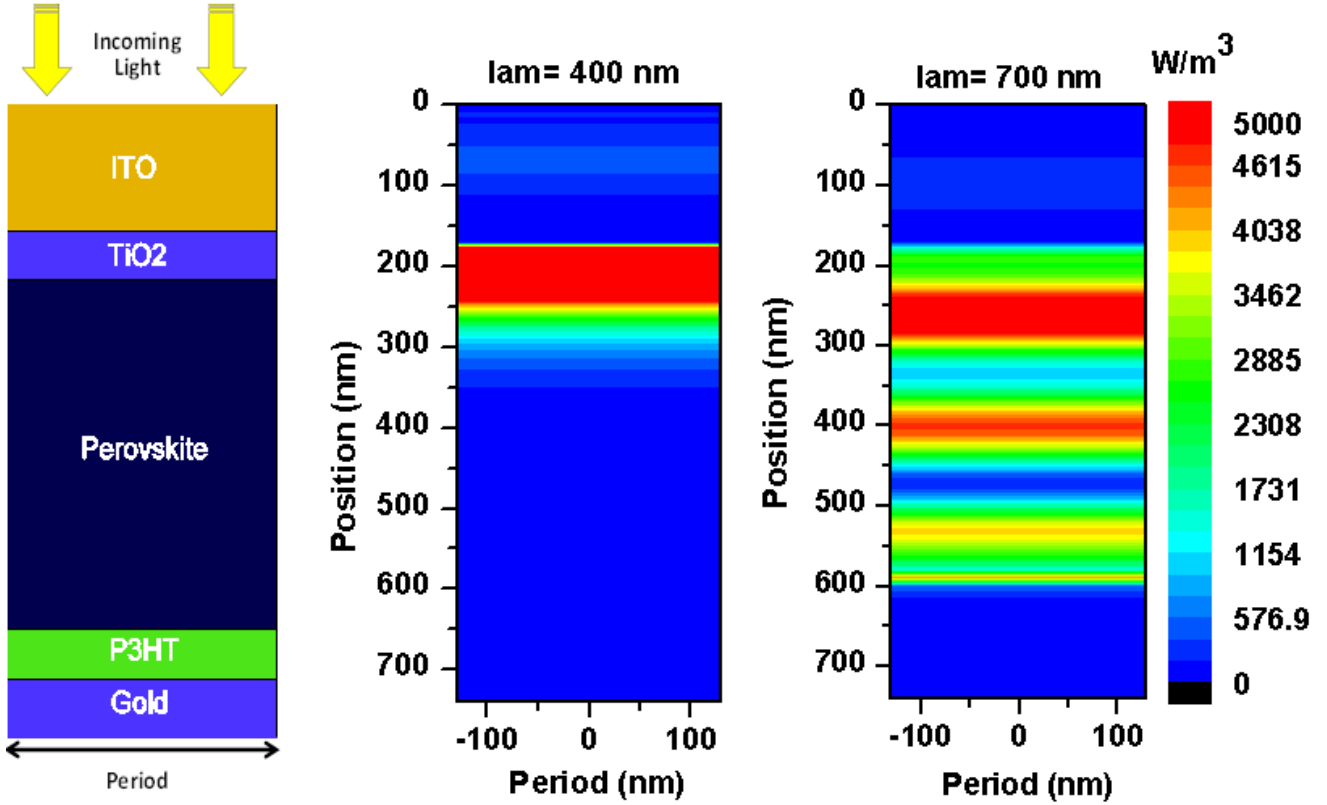


Figure 1. (a) Schematic cross section of simulated perovskite solar cell on smooth substrate; corresponding power loss profile for monochromatic illumination of wavelength (b) 400 nm, and (c) 700 nm

Figure 1(a) displays the reference cell structure of the solar cell. The complex refractive indices for each layer were used to simulate the electric field distribution throughout the device structure. The simulations of the optical wave propagation within the solar cell were carried out for wavelengths ranging from 300 nm to 800 nm. From the electric field distribution, power loss for the individual regions of the solar cell were calculated by using the equation (1).

$$Q(\mathbf{x}, \mathbf{z}) = \frac{1}{2} \mathbf{c} \epsilon_0 \mathbf{n} \alpha |\mathbf{E}(\mathbf{x}, \mathbf{z})|^2 \quad (1)$$

where α is the absorption coefficient, $E(x, z)$ is the electric field, n is the refractive index of materials, c is the light velocity in the free space, and ϵ is the permittivity of free space.

The time average power loss map within p-i-n superstrate configuration solar cell is shown in Figure 1(b) and 1(c). The incident wavelengths were 400 nm and 700 nm. It was calculated for an incident wave with an amplitude of 1 V/m. For the shorter wavelengths, $\text{CH}_3\text{NH}_3\text{PbI}_3$ has higher extinction or absorption coefficient. As a consequence, most of the lights are absorbed at the interface of TiO_2 and $\text{CH}_3\text{NH}_3\text{PbI}_3$ layer and then some of the light is absorbed in the bulk of the

active layer. However, very few power loss was observed at ITO, TiO_2 , and P3HT due to the presence of a small optical behavior in shorter wavelengths. Whereas, the absorption in the absorbing perovskite layer in 700 nm is comparatively higher than 400 nm since the extinction coefficient for the $\text{CH}_3\text{NH}_3\text{PbI}_3$ material is very high and it absorbs the maximum incoming light for the red or infrared red part of wavelength spectrum. Although ITO and TiO_2 are almost transparent for longer wavelengths of optical spectrum, there is a small amount of parasitic absorption loss in P3HT and its total loss can be calculated as almost 8.15%.

In organic-inorganic halide perovskite solar cells, the internal quantum efficiency is assumed to be 100%. Therefore, the determined quantum efficiency defines an upper limit of the achievable external quantum efficiency. The quantum efficiency for a perovskite solar cell can be calculated as the ratio of the power absorbed in the perovskite absorber material to the total power incident (P_{Opt}) on the unit cell. The following equation (2) was used to calculate the quantum efficiency:

$$QE = \frac{1}{P_{\text{Opt}}} \int Q(\mathbf{x}, \mathbf{y}) d\mathbf{x} d\mathbf{y} \quad (2)$$

The short circuit current was calculated based on the external quantum efficiency using the following equation (3):

$$I_{SC} = \frac{q}{hc} \int_{\lambda_{min}}^{\lambda_{max}} \lambda \cdot QE(\lambda) \cdot S(\lambda) d\lambda \quad (3)$$

where h is Planck's constant, c is the light velocity, q is the elementary charge, λ is the wavelength, and $S(\lambda)$ is the spectral irradiance of sunlight (AM 1.5).

3. Optimization of Perovskite Solar Cell

In order to optimize i.e., to maximize the short circuit current and quantum efficiency of the perovskite solar cell on smooth substrate, the influence of the variation of thickness of TiO_2 , $CH_3NH_3PbI_3$, and P_3HT layers on quantum efficiency and short circuit current was studied using the FDTD method.

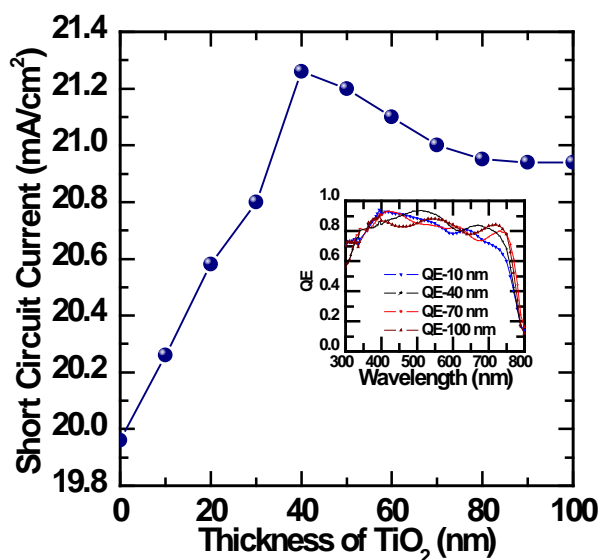


Figure 2. Short circuit current as a function of the thickness of TiO_2 . Corresponding comparison of quantum efficiency for perovskite based solar cell with the variation of TiO_2 layer thickness (Inset)

TiO_2 layer thickness was varied in between 0 nm and 100 nm, while perovskite layer and other layer thicknesses were kept constant. The simulated short circuit current as a function of the TiO_2 layer thickness along with the external quantum efficiency as a function of wavelength range 300 - 800 nm (inset) are depicted in Figure 2. The variation of the TiO_2 layer thickness has a great influence on the short circuit current. The short circuit current increases with the increase of thickness up to 40 nm and it decreases and becomes almost saturated after 40 nm. This is due to the fact that the photon absorption in perovskite photoactive material for the red and infrared red part of light spectrum is very poor and most of the light is absorbed in the blue region (300 nm- 400 nm) below the 40 nm of the TiO_2 thickness. As the thickness increases the absorption increases mainly in the 600 nm- 800 nm of the wavelength spectrum. So, above the 40 nm thickness of the TiO_2 layer has hardly any influence on the device performance since its absorption in the visible range and the change of short circuit current are negligible and the reflection coefficient at the ITO/ TiO_2 interface is low so

that interference effects that depend on the TiO_2 thickness play a minor role. However, a maximum short circuit current density of 21.42 mA/cm^2 can be achieved at 40 nm of TiO_2 , having maximum about 92.4% of external quantum efficiency at 520 nm.

P_3HT is particularly used as a hole transport layer, which is also varied in 0 nm to 100 nm for the investigation. By varying the thickness of P_3HT layer, we actually vary the distance of the active region to the reflecting Au metal electrode since P_3HT has also absorption and carriers generation capability, thereby driving the active region through a pronounced interference pattern [9]. The calculated short circuit current density and external quantum efficiency (inset) are inscribed in Figure 3. At 10 nm thickness of ultrathin P_3HT layer, the short circuit current density and quantum efficiency are maximum i.e., the photoactive region is placed at the maximum of the optical field distribution and the short circuit current has a maximum value of 21.9 mA/cm^2 . With increasing P_3HT thickness the short circuit current decreases, having a minimum value of about 20.5 mA/cm^2 at 100 nm of thickness. However, the photon absorption in the absorbing material decreases with the increase of the layer thickness, especially in the longer wavelengths (600 - 750 nm).

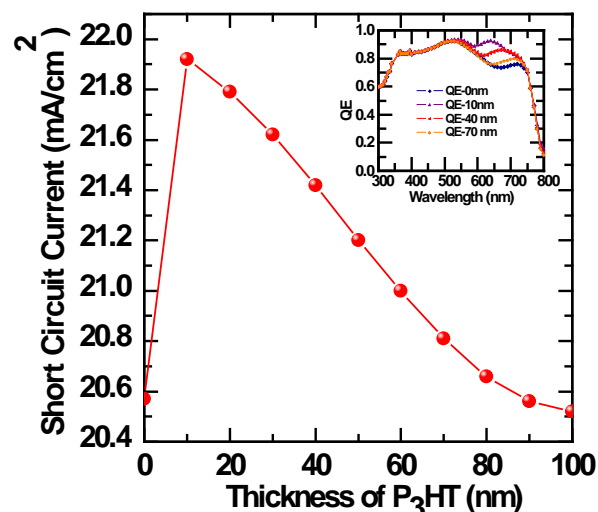


Figure 3. Short circuit current as a function of the thickness of P_3HT . Corresponding comparison of quantum efficiency for perovskite based solar cell with the variation of P_3HT layer thickness (Inset)

The influence of the perovskite absorber layer thickness on the short circuit current and the quantum efficiency (inset) is shown in Figure 4. The thickness of the $CH_3NH_3PbI_3$ layer was varied from 100 nm to 600 nm, whereas thickness for other layers were kept constant. As the thickness of the perovskite layer is increased, a significant increase of the short circuit current as well as the quantum efficiency was observed. For a solar cell active layer thickness of 600 nm, the short circuit current increases from around 15.5 mA/cm^2 to 22.7 mA/cm^2 . A significant amount of light absorption is also observed almost in the whole wavelength spectrum (450 nm- 750 nm) depicted in Figure 4 (inset). But we cannot merely increase the thickness of the absorber material due to the shorting defects that arises from the large crystals and it might create additional defects in the band gap acting as recombination centers for photogenerated carriers, which in turn deteriorates its electrical properties [8]. Hence 360

nm perovskite layer has been predicted as the optimum thickness for the further investigation.

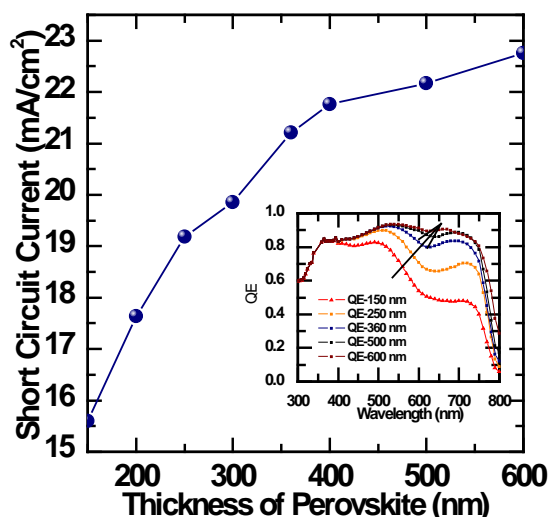


Figure 4. Short circuit current as a function of the thickness of perovskite ($\text{CH}_3\text{NH}_3\text{PbI}_3$) layer. Corresponding comparison of quantum efficiency for perovskite based solar cell with the variation of perovskite layer thickness (Inset)

The optimization process of perovskite planar solar cell structure has been carried out by mainly observing the influence of thickness for different layers of the cell. Based on the best short circuit current and quantum efficiency, an optimal solar cell layer sequence, ITO(130 nm)/ TiO_2 (40 nm)/ $\text{CH}_3\text{NH}_3\text{PbI}_3$ (360 nm)/ P_3HT (10 nm)/Au (100 nm), has been obtained. The optimal flat solar cell structure leads to an increase of the short circuit current by 0.26 mA/cm^2 , resulting in a short circuit current density of 22.05 mA/cm^2 . The quantum efficiency plot for the optimized perovskite solar cell with smooth surface along with parasitic absorption losses in different layers are depicted in Figure 5. The optimal structure exhibits an advantage of the quantum efficiency in the region of 550 nm - 700 nm, since the structure was adjusted by obtaining mainly the best thickness of P_3HT layer which has better absorption in that region.

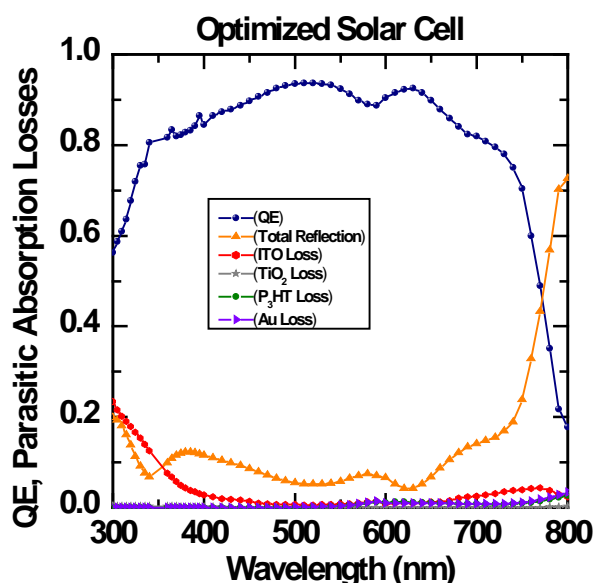


Figure 5. Quantum Efficiency and Parasitic absorption losses of optimized perovskite based thin-film solar cell

The optimized cell has a very low absorption in the TiO_2 , P_3HT , and Au compared to ITO. The maximum quantum efficiency about 93% can be obtained in 490 nm-540 nm of wavelength spectrum. In terms of the parasitic absorptions, the ITO, TiO_2 , P_3HT , and Au metal layers absorb 0.62%, 0.028%, 0.067 %, and 0.11 %, respectively at 510 nm, whereas $\text{CH}_3\text{NH}_3\text{PbI}_3$ absorbs almost 93.7% of the total absorbed light in the entire solar cell stack. The largest loss is observed for ITO layer mainly for the shorter wavelengths (300 – 400 nm), while it is almost transparent in 400 nm - 700 nm of optical spectral range. However, the total optical loss increases for the longer wavelengths though it is very low for the shorter wavelengths. The reflection can be calculated as $R = 1 - A$, where A is the total absorption of the solar cell. It can be observed that the upper portion of the quantum efficiency curve is white, representing the total reflection from the solar cell.

4. Comparative Analysis of $\text{CH}_3\text{NH}_3\text{PbI}_2\text{Cl}$ and $\text{CH}_3\text{NH}_3\text{PbI}_3$ Perovskite Solar Cells

In this section, the comparison of $\text{CH}_3\text{NH}_3\text{PbI}_3$ and $\text{CH}_3\text{NH}_3\text{PbI}_2\text{Cl}$ based perovskite thin-film solar cell was studied. The comparison was carried out based on the simulated quantum efficiency, short circuit current density, and parasitic absorption losses in each layer. A comparative short circuit current and quantum efficiency plots are depicted in Figure 6(a) and Figure 6(b). By using $\text{CH}_3\text{NH}_3\text{PbI}_2\text{Cl}$ perovskite photoactive material, an enhancement of quantum efficiency is pronounced in the longer wavelengths (700 nm- 800 nm) due to the better incoupling of light to the absorber layer. Moreover, the diffusion length of the $\text{CH}_3\text{NH}_3\text{PbI}_2\text{Cl}$ perovskite absorber is much more higher than $\text{CH}_3\text{NH}_3\text{PbI}_3$ perovskite material, which enhances the volume of the space charge region and increases size of the effective thickness, therefore allowing more carriers to be dissociated into free charges. However, for the shorter wavelengths (300 nm-700 nm) there is no significant difference of light absorption in the active layer between $\text{CH}_3\text{NH}_3\text{PbI}_2\text{Cl}$ and $\text{CH}_3\text{NH}_3\text{PbI}_3$ perovskite solar cell. Compared to the short circuit current values obtained for $\text{CH}_3\text{NH}_3\text{PbI}_3$ solar cell over the variation of the absorber layer thickness, the current values calculated from $\text{CH}_3\text{NH}_3\text{PbI}_2\text{Cl}$ perovskite solar cell is higher by around 2.5% almost all the way in the range from 360 nm to the 700 nm thickness of the absorbing layer.

The short circuit current gain can be calculated as about 0.40 mA/cm^2 . This is due to the fact that the carrier lifetime along with multiple passes or bounces of incident light ray increases by using $\text{CH}_3\text{NH}_3\text{PbI}_2\text{Cl}$, consequently the absorption in the absorber layer increases as well. Moreover, the parasitic absorption losses are drastically decreased in the hole transport layer (P_3HT) and back contact (Au) layer of the solar cell as inscribed in Figure 7 (c) & (d). The parasitic absorption loss in the P_3HT layer for the $\text{CH}_3\text{NH}_3\text{PbI}_3$ perovskite solar cell was calculated as 9.04%, whereas it is only 5.7% for $\text{CH}_3\text{NH}_3\text{PbI}_2\text{Cl}$ perovskite solar cell in the 600 nm of wavelength. On an average about 2.18% of higher parasitic absorption loss is

pronounced in the Au layer for the $\text{CH}_3\text{NH}_3\text{PbI}_3$ perovskite solar cell, compared with $\text{CH}_3\text{NH}_3\text{PbI}_2\text{Cl}$ perovskite solar cell mainly in the longer wavelengths

(600 nm- 800 nm). However, losses are almost same in the ITO and TiO_2 layer shown in Figure 7 (a) & (b).

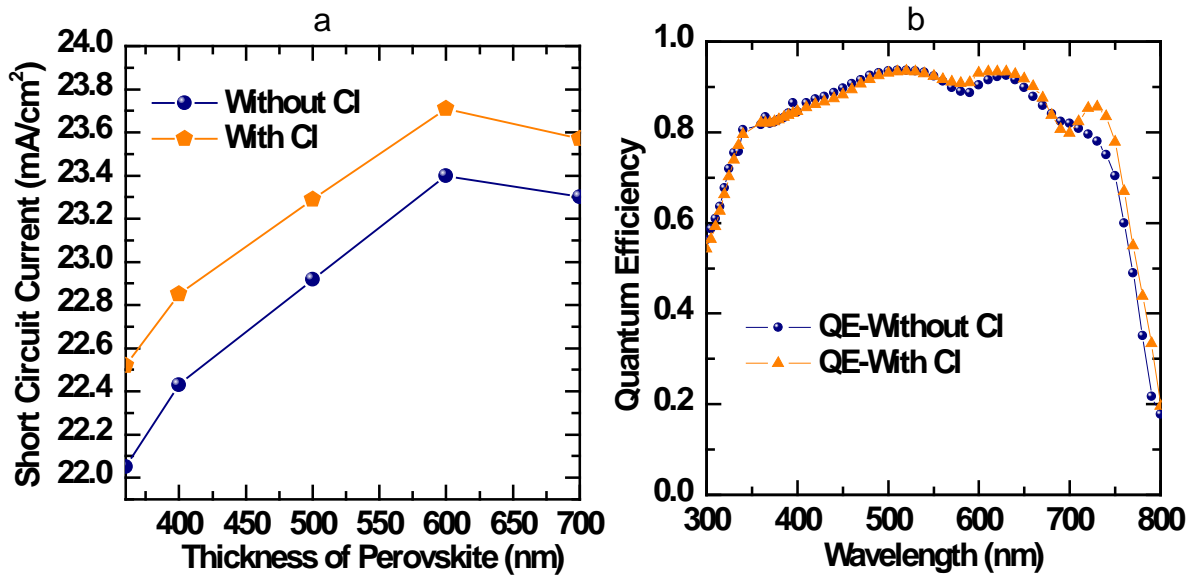


Figure 6. a) Comparison of short circuit current with the variation of perovskite based thin film solar cell with and without Cl; b) Comparison of quantum efficiency plots for 360 nm of perovskite based thin film solar cell with and without Cl

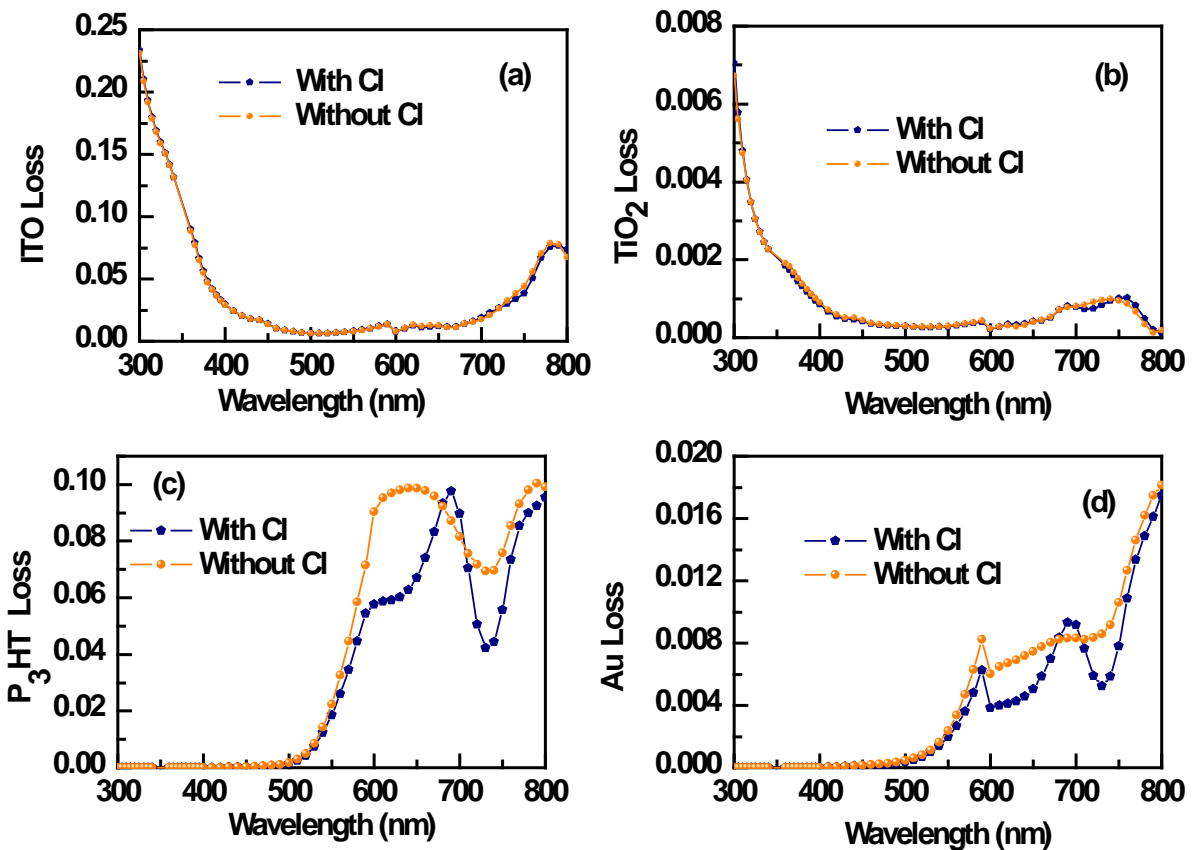


Figure 7. Comparison of parasitic absorption losses between $\text{CH}_3\text{NH}_3\text{PbI}_2\text{Cl}$ and $\text{CH}_3\text{NH}_3\text{PbI}_3$ perovskite based thin-film solar cells in a) ITO, b) TiO_2 , c) P_3HT , and d) Au layers

5. Conclusion

The study of thin-film perovskite photovoltaic cell was started with the optimization of simple planar surface solar cell by analyzing the influence of the variation of the

thickness in different layers on short circuit current and quantum efficiency using finite difference time domain (FDTD) method. The optimized cell achieves maximum of 22.05 mA/cm² short circuit current density with 93% of external quantum efficiency in the 530 nm of wavelength spectrum. P_3HT plays a major role in optimizing the cell since it exhibits an advantage of the quantum efficiency in

the region of 550 nm - 700 nm. It has also come to realize that the overall gain of the $\text{CH}_3\text{NH}_3\text{PbI}_2\text{Cl}$ based perovskite solar cell is higher than $\text{CH}_3\text{NH}_3\text{PbI}_3$ perovskite solar cell due to the higher carrier diffusion length, optical effective thickness, and absorption capability mainly in the longer wavelength range (700 nm-800 nm). However, the knowledge of optics studied in this research on this excellent perovskite thin-film solar cell can be implemented in high efficiency tandem devices. Since perovskite material could be used as an excellent top cell along with suitable Si material as bottom cell, which would link into existing, extensive research activities all over the world into high efficiency, back contact Si solar cells.

Acknowledgement

The authors would like to thank Prof. Dietmar Knipp, Dr. Rahul Dewan, and Dr. Vladislav Jovanov for their all kinds of support to learn the algorithm for the simulation. The lecture notes from the graduate course "Computational Electromagnetics" offered at Jacobs University Bremen, Germany by Prof. Jon Wallace was of great help for the formulation of the FDTD algorithm and understand the subject matter.

References

- [1] Kayes, B.M.; Hui Nie; Twist, R.; Spruytte, S.G.; Reinhardt, F.; Kizilyalli, I.C.; Higashi, G.S., "27.6% Conversion efficiency, a new record for single-junction solar cells under 1 sun illumination," in Photovoltaic Specialists Conference (PVSC), 2011 37th IEEE, vol., no., pp.000004-000008, 19-24 June 2011.
- [2] A. Kojima, K. Teshima, Y. Shirai, T. Miyasaka, *J. Am. Chem. Soc.* 131, 6050-6051 (2009).
- [3] Lotsch, B. V. (2014), New Light on an Old Story: Perovskites Go Solar. *Angew. Chem. Int. Ed.*, 53: 635-637.
- [4] Henry J. Snaith. Perovskites: The Emergence of a New Era for Low-Cost, High-Efficiency Solar Cells. *J. Phys. Chem. Lett.*, 2013, 4 (21), pp 3623-3630.
- [5] Lee, M. M., Teuscher, J., Miyasaka, T., Murakami, T. N. & Snaith H. J. Efficient hybrid solar cells based on meso-superstructured organometal halide perovskites. *Science* 338, 643-647 (2012).
- [6] Stranks, S. D. et al. Electron-hole diffusion lengths exceeding 1 micrometer in an organometal trihalide perovskite absorber. *Science* 342, 341-344 (2013).
- [7] Qianqian Lin, Ardalan Armin, Ravi Chandra Raju Nagiri, Paul L. Burn and Paul Meredith Electro-optics of Perovskite Solar Cells. *Nature Photonics*, Vol. 9, Feb. 2015.
- [8] Y. Kim, S. A. Choulis, J. Nelson, D. D. C. Bradley, S. Cook, J. R. Durrant, *Appl. Phys. Lett.* 2005, 86, 063502.
- [9] Victoria Gonzalez-Pedro, Emilio J. Juarez-Perez, Waode-Sukmawati Arsyad, Eva M. Barea, Francisco Fabregat-Santiago, Ivan Mora-Sero *, and Juan Bisquert*, "General Working Principle of $\text{CH}_3\text{NH}_3\text{PbX}_3$ Perovskite Solar Cells", *Nano Lett.*, 2014, 14 (2), pp 888-893.